Characterisation of the Mechanobiology of Stents *In Vitro*

Luke BOLDOCK [1, 2], Charlotte POITEVIN [1], Helen L CASBOLT [1], Sarah HSIAO [3], Paul C EVANS [3], Cecile M PERRAULT [1, 2*]

* Corresponding author: Tel.: +44 (0)114 2220154; Email: c.perrault@sheffield.ac.uk
1: Department of Mechanical Engineering, University of Sheffield, UK
2: INSIGNEO Institute for *In Silico* Medicine, University of Sheffield, UK
3: Department of Cardiovascular Science, University of Sheffield, UK

Abstract Long-term efficacy of percutaneous coronary intervention (PCI) to treat coronary heart disease is hampered by incidence of in-stent restenosis (ISR). The regrowth of a healthy endothelial layer post-treatment, a key factor in successful vascular repair, has been shown to be affected by the high sensitivity of endothelial cells (EC) to shear stress. Characterisation of stented artery haemodynamics is required to understand the response of EC to complex flow and shear stress patterns induced by stent structure. A device for the *in vitro* study of coronary stents has been developed and fabricated in polydimethylsiloxane (PDMS). Balloon-mounted cobalt-chromium stents have been successfully deployed, and particle tracking has been employed to obtain streamlines under low flow rate. High-resolution flow-patterns can be imaged, and complemented with *in silico* analysis from μCT data. The device allows for the seeding of EC, and sustained exposure to shear stress. EC response can be investigated by comparing real-time footage of cellular migration and proliferation to the haemodynamics of the specific region.

Keywords: flow mechanics, shear stress, *in vitro* assay, stent, cardiovascular disease

1. Introduction

Coronary heart disease is the leading cause of death worldwide, claiming 7 million lives annually (Mackay *et al*, 2004). Minimally invasive treatments are available to alleviate symptoms caused by atherosclerosis and stenosis, the narrowing and blocking of arteries. Percutaneous coronary intervention (PCI) widens stenosed arteries with inflatable balloon catheters, with the subsequent insertion of stents to act as supporting scaffolds. However, PCI with bare metal stents (BMS) has been associated with rates of ensuing in-stent restenosis of up to 44% (Farooq *et al*, 2011). Globally, more than 1.5 million people receive stents each year (McFadden *et al*, 2004). Optimising stented artery repair would reduce mortality and improve quality of life.

The development of ISR is initiated by denudation of the endothelium, the vessel's cellular lining, by balloon and stent expansion. This injury, in addition to the presence of the stent as a foreign body, leads to inflammation, migration of smooth muscle cells (SMC), neointimal hyperplasia, and ultimately ISR; defined as >50% reduction of luminal diameter (Kuntz *et al*, 1992).

Accordingly, several factors are deemed central in reducing ISR incidence: minimising the impact of stent deployment through considered design (Sangiorgi *et al*, 2007); reducing inflammation and SMC proliferation; minimising EC loss and promoting the regeneration of a healthy endothelium (Hamid and Coltart, 2007).

Current technological trends for improved stent performance focus on drug-eluting stents (DES), which release anti-proliferative agents to inhibit SMC and neointimal growth. While DES have been shown to reduce rates of ISR (Farooq *et al*, 2011), anti-proliferatives also act to inhibit endothelial repair (Chaabane *et al*, 2013). Furthermore, as peak neointimal growth is seen at 6-12 months post-treatment (Virmani *et al*, 2003), polymer coatings are required to reduce rates of elution, which are themselves known to cause inflammation

(Bangalore *et al*, 2013).

More recently, fully bioabsorbable stents have been developed and clinically trialled. Guidance on their use in the UK is due in May 2014 (National Institute for Health and Care Excellence, 2014), however, shortcomings have been noted (Waksman, 2006). Thicker, more impactful bioabsorbable polymer structures are required to provide the same stiffness as BMS, and ISR may still occur in the months prior to full dissolution.

A third approach considers the mechanical, haemodynamic environment of the stent/artery system. As described by Van der Heiden *et al* (2013), EC mechanoreceptors react to blood flow induced shear stress, differentiating between variations in magnitude and direction.

Low (0-4 dynes/cm^2 [0-0.4 Pa]) (Malek *et al*, 1999; Duraiswamy *et al*, 2007) or oscillatory shear stress inhibits reendothelialisation, with EC migration away from areas of significant shear stress gradient, consistent with the observation that regions of low shear stress, such as bifurcations, are particularly prone to atherosclerosis (Hoefer *et al*, 2013).

Conversely, high (~15 dynes/cm^2 [1.5 Pa]) (Sprague *et al*, 1997; Duraiswamy *et al*, 2007), uniform shear stress supports a healthy endothelium and conveys protective effects: the activation of genes reducing inflammation and thrombus formation, the inhibition of SMC proliferation (Ueba *et al*, 1997) and reduction of neointimal hyperplasia.

Promoting high, uniform shear stress and minimising areas of low or oscillatory shear stress should therefore be considered during efforts to prevent ISR. Full characterisation of the stented artery is required to understand the influence of shear stress on the endothelium and vascular repair.

Initial studies of stent structures used simple models. For example, Sprague *et al* (1997) implanted metal coupons on collagen gels which were seeded with EC and exposed to various flow conditions. While such techniques effectively illustrate the effect of shear stress, and have been more recently reemployed by Sprague *et al* (2012) to evaluate patterned stent surfaces, replication of the entire stent mesh and the vessel's tubular structure is necessary.

Benbrahim *et al* (1994; 1996) and Moore *et al* (1994) fabricated tubular structures within which EC were exposed to haemodynamic forces, and increasingly realistic vascular models have since been developed. Both realistic pulsatile flow (Peng *et al*, 2000) and the combined action of multiple forces (O'Cearbhaill *et al*, 2008) have been introduced.

Punchard *et al* built upon their own previous work, creating a silicone tube to assess seeded EC under haemodynamic conditions (2007), to create one of the first *in vitro* models into which a stent was deployed (2009). The device demonstrates an experimental approach required to assess the behavior of EC within the stented artery, although the assessment is limited to a single, static examination which necessitates destruction of the model.

This work aims to create a technique by which repeated use *in vitro* and *in silico* models can be utilised in combination to characterise the haemodynamics of complex stent structures; to observe the effects of modified shear stress on EC migration and proliferation in real-time; and to compare, quantify and predict the effects of commercial stent design on endothelial repair.

2. Materials and methods

In vitro model

Moulds were created by threading 80mm long straight sections of fluorinated ethylene propylene (FEP) tubing through the walls of 56mm diameter Petri dishes. 2mm and 3mm diameter tubing represented typical diameters of coronary arteries (Dodge *et al*, 1992).

PDMS (Sylgard 184, Dow Corning Corp., Midland, USA) was prepared by mixing base and curing agent at a 10:1 ratio by weight, and degassing in a vacuum desiccator. 22g was poured into each mould and cured, to create

9mm thick silicone elastomer blocks containing channels of circular cross-section.

Balloon catheters were guided into the tubular channels and inflated to deploy ready-mounted cobalt-chromium alloy stents (kindly contributed by the Royal Hallamshire Hospital, Sheffield). Stents of 8mm, 16mm and 19mm length, and 4mm nominal diameter were deployed. Inflation at 6 atm, to the minimum stated balloon diameter of 3.39mm, allowed catheters within 3mm diameter channels to meet the 'gold standard' balloon to artery ratio of 1.1 – 1.2:1. Catheters were withdrawn, and inspection under a microscope confirmed adequate stent expansion.

Stented channels are connected, via additional FEP tubing, to fluid reservoirs and a peristaltic pump to provide a constant pulsatile unidirectional flow. In addition to the appropriate selection of channel diameter and stent deployment procedure, flow rate and associated shear stress can be adjusted to attain conditions comparable to those *in vivo*.

Flow rates required to achieve desired levels of mean wall shear stress (τ_{mean}) were calculated using the Hagen-Poiseuille equation:

$$\tau_{mean} = \frac{4\mu Q}{\pi r^3}$$

where Q is the volumetric flow rate, μ the dynamic viscosity of the fluid and r the internal radius of the channel. Reynolds numbers were found, and used to confirm that channel entrance lengths were long enough for the flow to fully develop before reaching stent leading edges.

Initial testing was conducted at low shear stress levels, not exceeding 1 dyne/cm^2 (0.1 Pa), by applying a maximum flow rate of 5 ml/min (2mm diameter channel) and 16 ml/min (3mm diameter channel).

Flow imaging

The optical transparency of PDMS allows direct observation of fluid flow around the stent *in situ*. 1µl of 10µm diameter FluoSpheres (Life Technologies, Carlsbad, USA) was added to 10ml of room temperature deionised water and subsequently used to image the flow using light and fluorescent microscopy. A number of video recordings were made with 4x, 10x, 20x and 40x objective lenses at various locations on the stent mesh, including entry and exit.

Flow patterns and streamlines were obtained by separating recordings into their constituent frames and manually tracking particles between them. Image scale and frame rates were used to extrapolate rough velocity profiles.

In silico model

In silico analysis of the stented channels using computational fluid dynamic models is performed from *in vitro* devices. Models are created from images obtained by micro computed tomography (µCT).

A SkyScan 1172 µCT scanner (Bruker, Billerica, USA) is used to obtain virtual cross-sectional slices of expanded stents. This raw data, with 7.86µm voxel resolution, can then be processed to reconstruct a 3D model.

Although the wall of the tube may be imaged, omitting the PDMS minimizes artefacts and allows the extraction and reconstruction of a more precise model of the stent. The arterial wall will be recreated in finite element software (Morlacchi *et al*, 2011), and the model imported into computational fluid dynamics software for analysis.

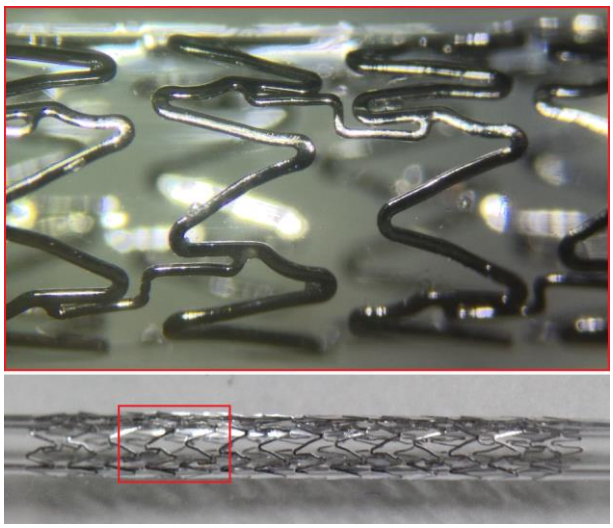

Figure 1: Structural detail of deployed stent

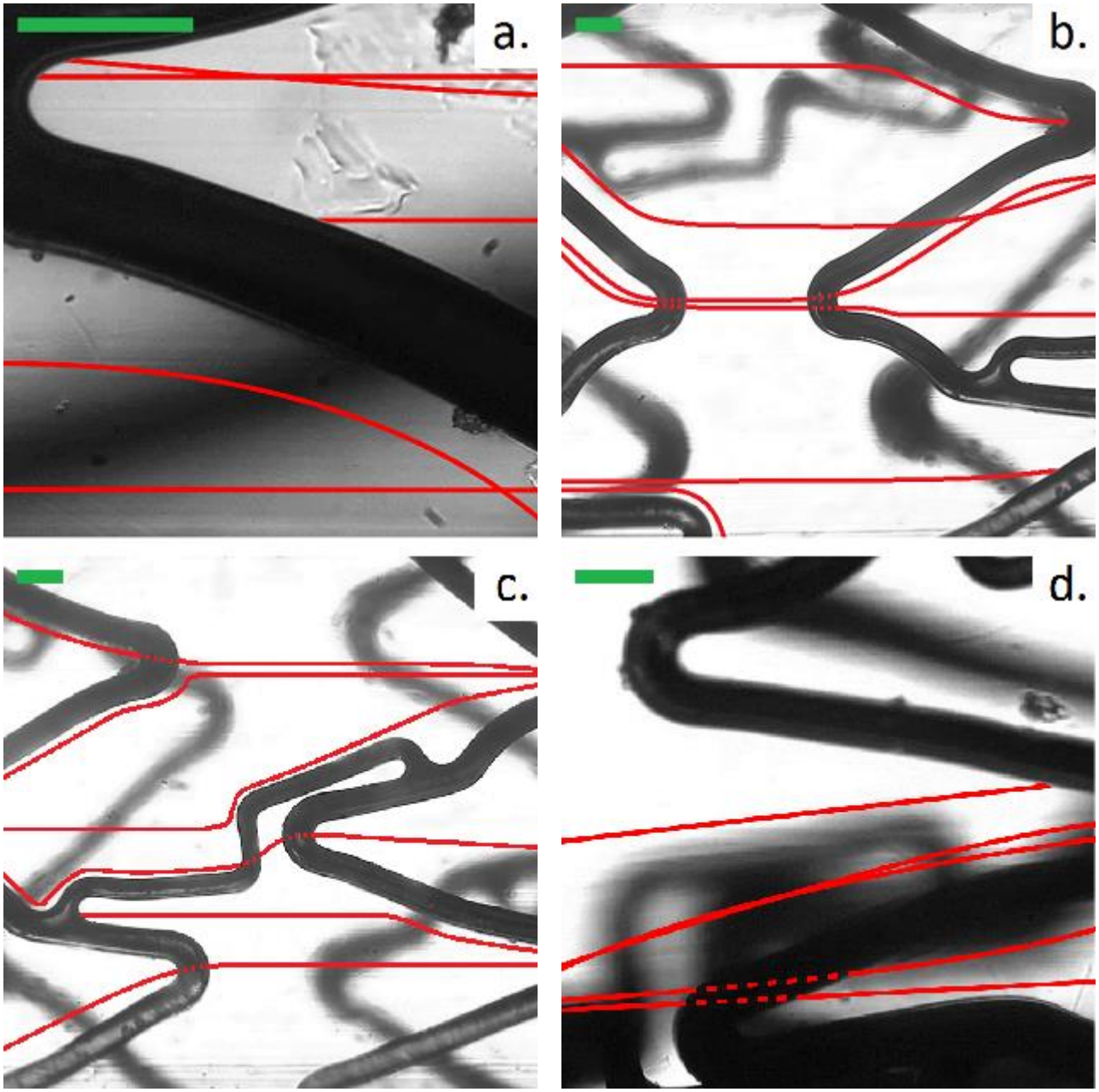

Figure 2: Tracked particle streamlines around stent struts. 4ml/min flow, left to right, 0.8 dynes/cm^2 (0.08 Pa). Scale bars: 100 µm.

3. Results

PDMS blocks containing circular channels were fabricated, and stents were successfully deployed. Visual inspection confirmed expansion and insertion into the channel wall. The structure of the expanded stent is illustrated in Fig. 1. 65µm struts are arranged in repeating offset peak-to-valley rings, connected by 3 bridges. The channels were readily connected to the reservoir and pump, and a range of low, physiologically comparable flows were applied.

Particle flow was visible under all magnifications. Light microscopy was favoured, as fluorescent microscopy did not show the local stent structure as a reference. A substantial velocity gradient was observed, fitting the profile expected of laminar pipe flow, i.e. increasing away from the wall.

Particles were seen to be influenced by the presence of the stent within ~150µm of the structure. As shown in Fig. 2, deviation from a laminar stream is revealed as particles are tracked along struts. Turbulent flow is further

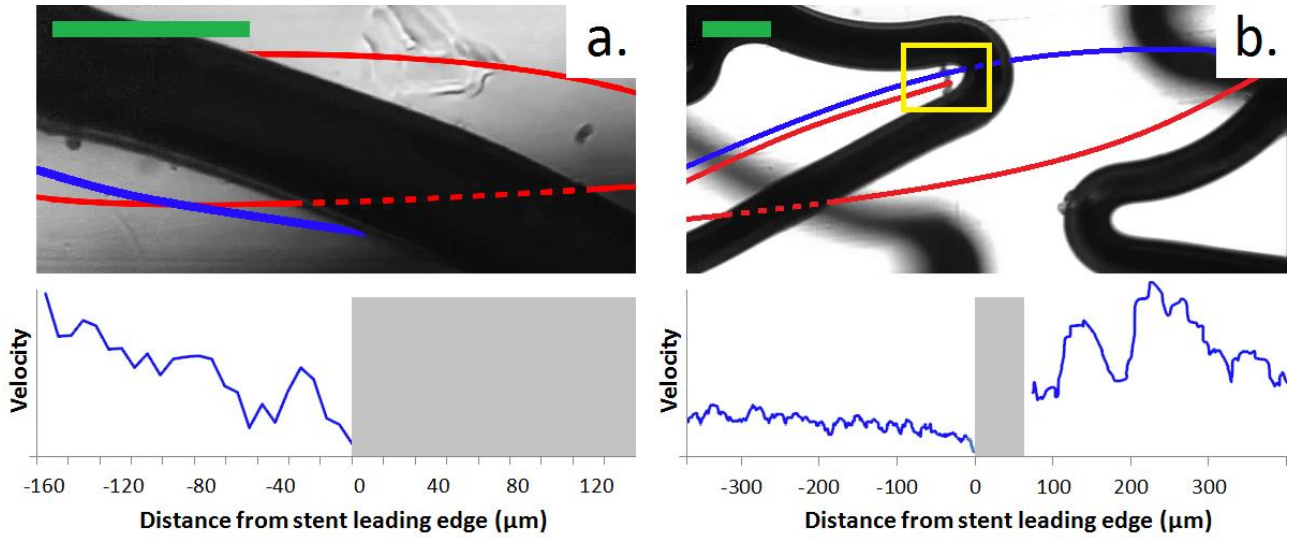

Figure 3: Estimated particle velocity profiles extracted from tracking data (blue streamline). 4ml/min flow, left to right, 0.8 dynes/cm^2 (0.08 Pa). Inset (b.) highlights area of particle accumulation.

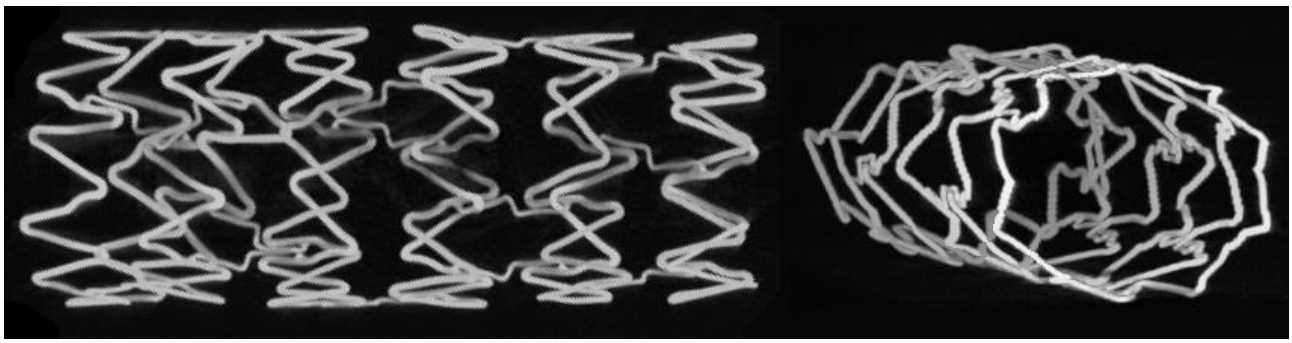

Figure 4: 3D reconstruction of stent from µCT data. 8mm long stent expanded to 3.39mm, within 3mm diameter channel.

indicated by deceleration towards, and acceleration away from, circumferentially orientated struts (Fig. 3). In some sites, particularly valleys in the ring structure, particles began to accumulate (Fig. 3 b.). Further observation and CFD may confirm whether these are areas of recirculation or stagnation points due to strut protrusion into the lumen.

µCT provided high-resolution data with minimal issue from image artefacts, from which a 3D model was reconstructed (Fig. 4).

3. Conclusion

We have created a novel microfluidic system for the study of stented arteries, recognizing the need for greater understanding of the system's mechanobiology. The use of PDMS rapid prototyping provided a customisable, cost- and time-efficient *in vitro* model. This allows high-throughput investigation of simple vascular anatomy, with the potential for modelling more complex structures, e.g. bifurcations and branch points.

In addition, the optical transparency of PDMS allowed the direct observation of flow using FluoSphere particles, demonstrating the complex patterns generated by stent structures.

Particle tracking velocimetry illustrated variable planar velocity; however, the method was not relied upon to provide quantitative data. The degree of uncertainty associated with scaling, the commercial recording and video-to-image conversion software, and human error in tracking was too great. The approach may be refined, although further work will indicate whether this current technique is at all practical when applied to the greater flow rates

required to test higher shear stress levels.

Particle tracking highlighted the benefit of performing CFD analysis in conjunction with *in vitro* modelling, for more accurate, quantitative results from three-dimensional data.

Following proof-of-concept presented here, the microfluidic system and biological compatibility of PDMS will enable the seeding and direct analysis of EC. Continuous flow of cell culture media around deployed stents, within the controlled environment of a microscope incubator, will allow migration and proliferation of EC to be observed first hand.

In vitro and *in silico* analysis can provide fluid dynamics data of far greater resolution that that possible with *in vivo* study, and real-time cellular monitoring improves on retrospective *ex vivo* examination. This combination will aid the full characterisation of stented artery haemodynamics over a greater range of shear stress levels, and the quantitative assessment and comparison of commercial stent designs.

Finally, this method could also be used for the development of new generations of DES, aligning drug diffusion patterns to observable effects on seeded EC. Assessment of the effects of shear stress on the dissolution of biodegradable stents and evaluation of the risk of embolism from non-uniform degradation are further examples of potential future applications of such research.

Acknowledgements

This work is supported by the University of Sheffield's Engineering for Life (E4L) and the MultiSim project (EP/K03877X/1), both funded by the Engineering and Physical Sciences Research Council.

References

Bangalore, S. *et al*, 2013. Bare metal stents, durable polymer drug eluting stents, and biodegradable polymer drug eluting stents for coronary artery disease: mixed treatment comparison. Br. Med. J. 347, f6625.

Benbrahim, A. *et al*, 1994. A compliant tubular device to study the influences of wall strain and fluid shear stress on cells of the vascular wall. J. Vasc. Surg. 20, 184-194.

Benbrahim, A. *et al*, 1996. Characteristics of vascular wall cells subjected to dynamic cyclic strain and fluid shear conditions in vitro. J. Surg. Res. 65, 119-127.

Chaabane, C. *et al*, 2013. Biological responses in stented arteries. Cardiovasc. Res. 99, 353-363.

Dodge, J.T. *et al*, 1992. Lumen diameter of normal human coronary arteries. Influence of age, sex, anatomic variation, and left ventricular hypertrophy or dilation. Circulation 86, 232-246.

Duraiswamy, N. *et al*, 2007. Stented artery flow patterns and their effects on the artery wall. Annu. Rev. Fluid Mech. 39, 357-382.

Farooq, V. *et al*, 2011. Restenosis: delineating the numerous causes of drug-eluting stent restenosis. Circ. Cardiovasc. Interv. 4, 195-205.

Hamid, H. and Coltart, J., 2013. Miracle stents – a future without restenosis. McGill J. Med. 10, 105-111.

Hoefer, I.E. *et al*, 2013. Biomechanical factors as triggers of vascular growth. Cardiovasc. Res. 99, 276-283.

Kuntz, R. *et al*, 1992. The importance of acute luminal diameter in determining restenosis after coronary atherectomy or stenting. Circulation 86, 1827-1835.

Mackay, J. and Mensah, G., 2004. The Atlas of Heart Disease and Stroke. 48-49. World Health Organisation.

Malek, A.M. *et al*, 1999. Hemodynamic shear stress and its role in atherosclerosis. JAMA 282, 2035-2042.

McFadden, E.P. *et al*, 2004. Late thrombosis in drug-eluting coronary stents after discontinuation of antiplatelet therapy. Lancet 364, 1519-1521.

Moore, J.E. *et al*, 1994. A device for subjecting vascular endothelial cells to both fluid shear stress and circumferential cyclic stretch. Ann. Biomed. Eng. 22, 416-422.

Morlacchi, S. *et al*, 2011. Hemodynamics and in-stent restenosis: micro-CT images, histology, and computer simulations. Ann. Biomed. Eng. 39, 2615-2626.

National Institute for Health and Care Excellence, 2014. Bioresorbable stent implantation for coronary artery disease: consultation document.

O'Cearbhaill, E.D. *et al*, 2008. Response of mesenchymal stem cells to the biomechanical environment of the endothelium on a flexible tubular silicone substrate. Biomaterials 29, 1610-1619.

Peng, X. *et al*, 2000. In vitro system to study realistic pulsatile flow and stretch signaling in cultured vascular cells. Am. J. Physiol. Cell Physiol. 279, C797-805.

Punchard, M.A. *et al*, 2007. Endothelial cell response to biomechanical forces under simulated vascular loading conditions. J. Biomech. 40, 3146-3154.

Punchard, M.A. *et al*, 2009. Evaluation of human endothelial cells post stent deployment in a cardiovascular simulator in vitro. Ann. Biomed. Eng. 37, 1322-1330.

Sangiorgi, G. *et al*, 2007. Engineering aspects of stent design and their translation into clinical practice. Ann. Ist. Super. Sanita 43, 89-100.

Sprague, E.A. *et al*, 1997. Human aortic endothelial cell migration onto stent surfaces under static and flow conditions. J. Vasc. Interv. Radiol. 8, 83-92.

Sprague, E.A. *et al*, 2012. Impact of parallel micro-engineered stent grooves on endothelial cell migration, proliferation, and function: an in vivo correlation study of the healing response in the coronary swine model. Circ. Cardiovasc. Interv. 5, 499-507.

Ueba, H. *et al*, 1997. Shear stress as an inhibitor of vascular smooth muscle cell proliferation – role of transforming growth factor-beta 1 and tissue-type plasminogen activator. Arterioscler. Thromb. Vasc. Biol. 17, 1512-1516.

Van der Heiden, K. *et al*, 2013. The effects of stenting on shear stress: relevance to endothelial injury and repair. Cardiovasc. Res. 99, 269-275.

Virmani, R. *et al*, 2003. Drug eluting stents: are human and animal studies comparable? Heart 89, 133-138.

Waksman, R., 2006. Biodegradable stents: they do their job and disappear. J. Invasive Cardiol. 18, 70-74.